6B.8

OCEAN-SURFACE WIND IMPACTS ON HURRICANE FORECASTNG: REGIONAL AND GLOBAL EXAMPLES

S. M. Leidner[1]*, J. Ardizzone[2], J. C. Jusem[3], E. Brin[2], R. N. Hoffman[1] and R. Atlas[4]
[1] Atmospheric and Environmental Research, Inc., Lexington, Massachusetts USA
[2] SAIC, Greenbelt, Maryland USA
[3] GEST, University of Maryland, Baltimore County, Maryland
[4] NOAA/Atlantic Oceanographic and Meteorological Laboratory (AOML), Miami, Florida USA

1. INTRODUCTION

Weather forecasting more than two days ahead is an inherently global problem. Synoptic weather systems propagate through regional modeling domains within 1-2 days, and the influence of the lateral boundaries becomes dominant thereafter. While the resolving power of global models continues to increase, now nearly into the mesoscale with the 16 km T1279 ECMWF model becoming operational on 26 January 2009, the small spatial scale of phenomena responsible for the intensification of tropical weather systems demands kilometer-scale, limited-area models. So the interaction between global and regional models continues to be critically important for hurricane forecasting beyond 2 days. In this study, we examine the impact of ocean surface wind data and the interaction of regional and global models on hurricane forecasting for Hurricanes Hanna and Ike of 2008.

2. EXPERIMENT DESIGN

Cycling data assimilation experiments using combinations of ocean surface wind data sets with the GEOS-5 system have been conducted. See Rienecker et al. (2008) for a description of the GEOS-5 system. The experiments use different combinations of QuikSCAT, ASCAT, SSMI and WindSat data, in addition to observations from a large compliment of *in situ* observing systems. In this report we focus on the impact of assimilating QuikSCAT and ASCAT vector winds on 5-day regional forecasts in the experiments listed in Table 1.

Exp. ID	***Name***	***Storms***
Control	Control (conventional observations)	Hanna/Ike
QSCAT	Control + QuikSCAT	Ike
ASCAT	Control + ASCAT	Hanna

Table 1. Data assimilation treatments presented in this paper.

The GEOS-5 Data Assimilation System (DAS) uses the Grid-point Statistical Interpolation (GSI, Kleist et al., 2009) method for data assimilation which allows for a non-homogeneous and anisotropic formulation of the background error covariance. GEOS-5 analyses are generated every six hours on the synoptic times (00, 06, 12 and 18 UTC) at 1°×1° horizontal resolution, and five day forecasts are generated from the 00 UTC analyses each day. These five-day forecasts are used to supply first guess fields and lateral boundary conditions for regional assimilation and forecast experiments with the WRF. Figure 1 illustrates the coordination between the GEOS-5 and regional forecasts using WRF. Additional GEOS-5 forecasts were generated as needed to supply lateral boundary conditions for the WRF experiments beginning at times other than 00 UTC.

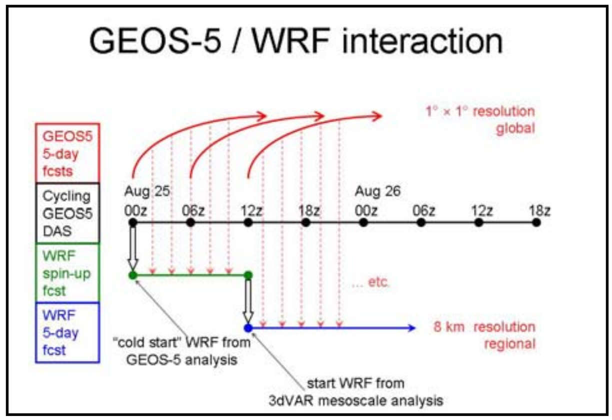

Figure 1: Illustration of the interaction between the global model (GEOS-5) and regional model (WRF-ARW) used in data assimilation this study.

For the WRF experiments reported here, we used a horizontal grid spacing of 8 km to take advantage of the high-resolution ocean surface wind data under examination. The WRF 3dVAR data assimilation system as configured for this study uses the slightly inhomogeneous and anisotropic background error covariances generated by Wu et al. (2002). While the GEOS-5 model and associated GSI data assimilation method are tuned to operate globally using a wide variety of observing systems, the WRF is a relocatable regional model with many options for assimilating observations and required some tuning. (a) A wind direction quality control check was added for QuikSCAT and WindSat retrieved winds (observation rejected if $|\Phi_{satellite}-\Phi_{background}|$ is greater than 80°). (b) The background error covariance horizontal length scales were tuned to 20% (80 km) of the default value (400 km) to accommodate the length scales of motion on a mesoscale grid. (c) Background error covariance magnitudes were reduced significantly (95%) to increase the influence of the "first guess" field, since default values badly overfit the observations at a resolution of 8 km.

* *Corresponding author address:* S. Mark Leidner, Atmospheric and Environmental Research, Inc., 350 David L. Boren Blvd., Suite 1535, Norman, Oklahoma 73072 USA; e-mail: leidner@aer.com.

The two hurricanes examined with this combined global/regional forecast design, Hurricanes Hanna and Ike (both 2008) were very different in character and provide independent cases for examining the impacts of ocean surface winds. The modeling domain for Hanna and Ike is shown in Figure 2.

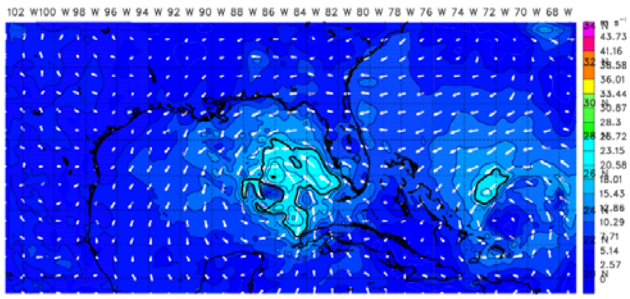

Figure 2. WRF 8 km resolution model domain used in this study for hurricanes Hanna and Ike. Ten-meter wind speed is plotted in colors consistent with AOML H*WIND analyses for 18 UTC 31 August 2008. Hurricane Gustav can be seen to the west of Florida, and Tropical Storm Hanna is southeast of the Bahamas.

Hurricane Hanna was a weak, meandering system, while Ike was a powerful, damaging storm whose track was driven decisively by the synoptic environment, straight into Galveston Bay. The results reported here are from GEOS-5 and WRF forecasts listed in Table 1 and initiated at 18 UTC 31 August 2008 (Hanna) and 00 UTC 12 September 2008 (Ike).

3. HURRICANE HANNA RESULTS

Figure 3 shows the best track path of Hurricane Hanna. Hanna was a long-lived tropical system that was never stronger than a category 1 hurricane during its lifetime. In the 3 days immediately after the experiment start time, Hanna executed a slow,

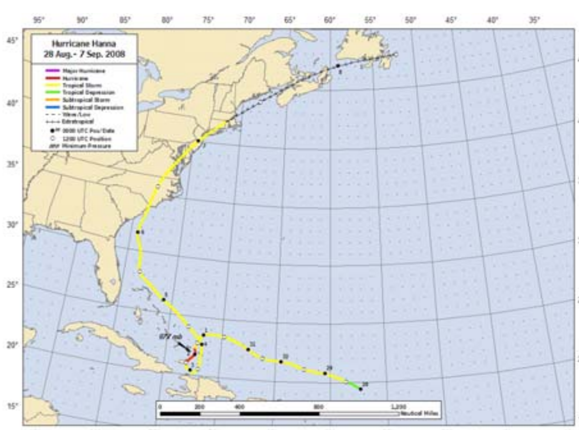

Figure 3. Best track chart of Hurricane Hanna (from NHC final report, Brown and Kimberlain, 2008).

counterclockwise loop (green track in Fig. 4) and deepened to 977 hPa (on 00 UTC 2 September). Hanna was then picked up by northerly steering currents, weakened by shear, and moved steadily toward the southeast U.S. Coast as a tropical storm.

Hanna presents a forecast challenge with respect to track and intensity. The steering forces during the 5-day forecast period shift from a large-scale, ridge building over the southeast U.S., to a strengthening of the sub-tropical ridge in the western Atlantic. The shear environment was also quite dynamic during this period, allowing Hanna to briefly reach minimal hurricane strength, only to be torn apart by shear over the next 12 hours (Brown and Kimberlain, 2008). Track error statistics (Fig. 5) show that ASCAT has the smallest overall position error, particularly for forecast days 3-5.

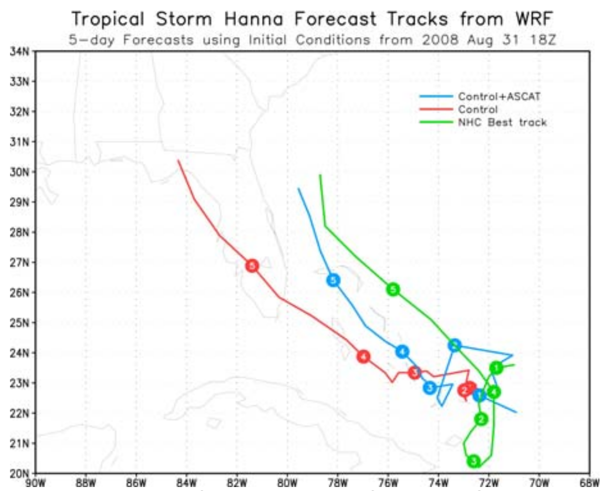

Figure 4. WRF forecast tracks from the Control and ASCAT treatments (red and blue lines, respectively) and the best track positions (green). 00 UTC positions are annotated with the day of the month in the colored circles.

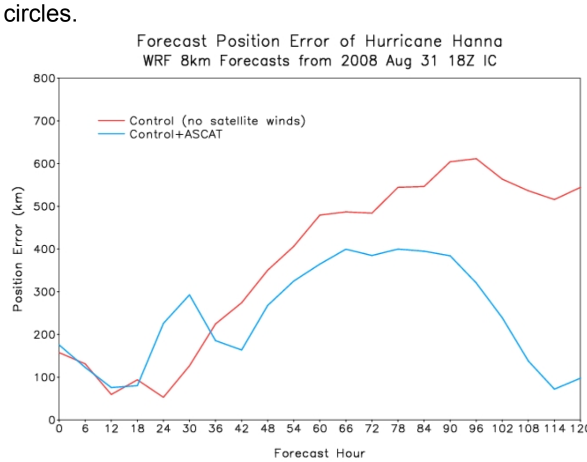

Figure 5. WRF track errors for Hanna experiments.

Regarding intensity, the WRF model deepened Hanna far too much, producing a major hurricane in both treatments (see Fig. 6). The significant environmental shear thought to have kept Hanna at tropical storm strength for most of its life may not have been well represented in the WRF. But why is the ASCAT forecast track so much better? For answers, we look to the impact of ASCAT data on the initial conditions and forecast.

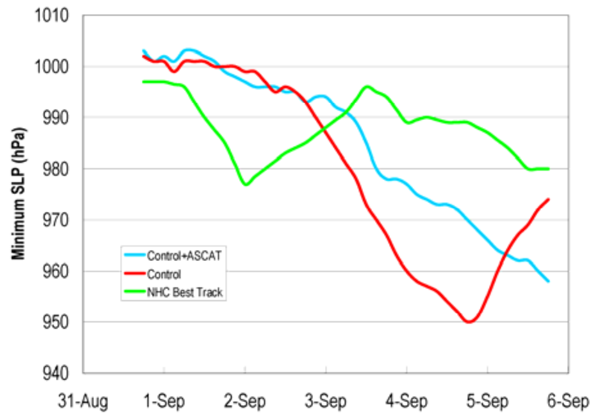

Figure 6. Minimum sea-level pressure traces for WRF forecasts and best track (green) of Hurricane Hanna.

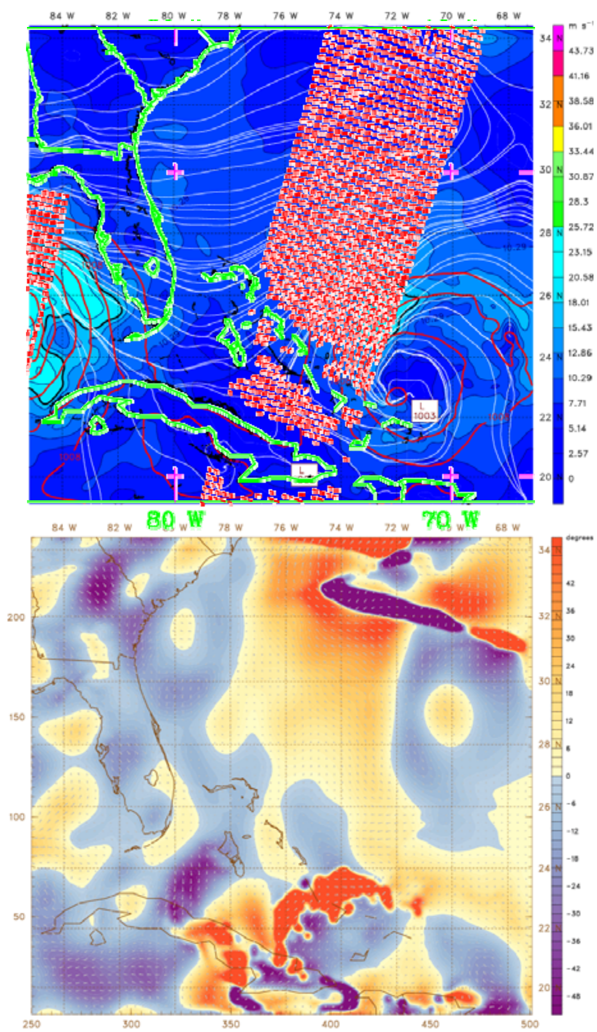

Figure 7. ASCAT analysis impacts. Upper panel: analyzed 10 meter wind speed for tropical storm Hanna, valid 18 UTC 31 August 2008 (colored field), wind streamlines (white), mean sea-level pressure (red contours) and ASCAT satellite wind locations (red markers). Lower panel: wind direction analysis increments (colored field), and vector increments (gray vectors).

The ASCAT overpass of tropical storm Hanna near 18 UTC 31 August provided scatterometer observations for part of the storm circulation (see satellite swath in Fig. 7, upper panel). The background has Hanna 175 km north of the observed center resulting in significant wind direction errors. For example, the ASCAT data reduced the wind on the northwest side of Hanna by 1-2 m/s, and changed the wind direction from northeasterly to more northerly flow. Both effects are consistent with the position error noted in the background. Unfortunately, too little of the circulation was observed by the ASCAT pass to permit relocation of the center closer to the observed position. Away from Hanna, the ASCAT data produced widespread wind direction changes and only minor adjustments to the wind speed (see Fig 7, lower panel). The wind direction increments seen in the lower panel of Fig. 7 were “carried away” by easterly winds and there was little evidence of their impact on Hanna after 18-24 hours.

One persistent difference between the Control and ASCAT forecasts, however, was the wind direction of the inflow at the northern boundary of the domain over the western Atlantic (not shown). The ASCAT experiment inflow wind direction was from the north and northwest over the 5-day forecast period, while the Control experiment inflow wind direction was from the north and northeast. The conditions flowing into the domain from the north affected the environment through which Hanna moved during the forecast. The only possible source for such a difference between the Control and ASCAT experiments is the GEOS-5 forecast fields which have been influenced by ASCAT data. Characterization of the differences in the steering currents or thermodynamic environments between Control and ASCAT experiments has not been conducted yet, nor have the specific ASCAT impacts within GEOS-5. But this work will be pursued to identify specific causes for the differences.

4. HURRICANE IKE RESULTS

Hurricane Ike was a powerful and historically damaging storm, mostly from the storm surge in Galveston Bay. Figure 8 shows the best track of Ike. The expected track was well-determined some days before landfall by the large-scale synoptic forcing. The challenge for Hurricane Ike is forecasting its intensity at landfall and the time of landfall.

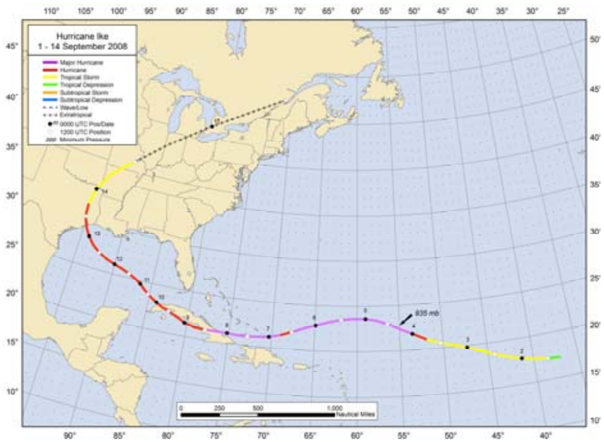

Figure 8. Best track chart of Hurricane Ike (from NHC final report, Berg, 2009).

Ike forecasts begin at 00 UTC 12 September, when the storm was a mature hurricane, and would make landfall just 30 hours later as a strong category 2 storm in Galveston. The best track estimates of minimum central pressure and maximum winds (see Fig. 9) show that Ike strengthened in the 9 hours just prior to landfall.

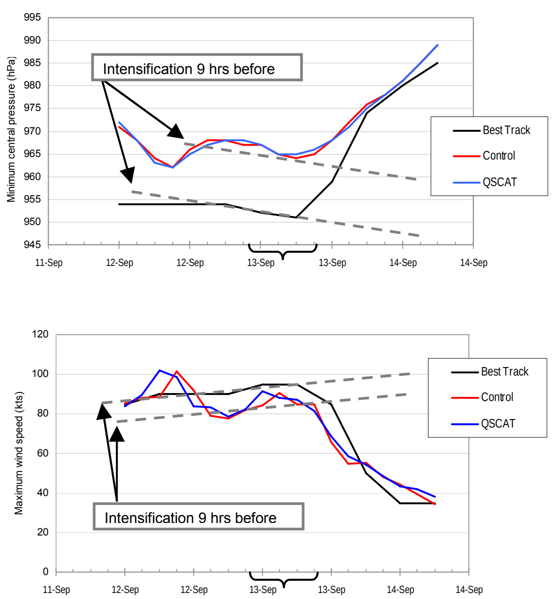

Figure 9. Minimum central pressure (upper panel) and maximum wind speed (lower panel) for Hurricane Ike, beginning 30 hours before landfall through 12 hours after landfall. The dashed lines in both panels indicate that the intensification rate 9 hours before land fall observed in the best track data is also seen in the WRF experiments.

The WRF forecasts show that Ike strengthens in the 9 hours before landfall (see gray dashed lines in Fig. 9), but the forecast central pressures were not nearly as deep as the best track.

The surface wind field at landfall contributed to considerable storm surge damage. Figure 10 shows the analyzed wind field from the AOML/HRD H*WIND analysis package (REFERENCE). As expected, winds are strongest to right of the hurricane track. The wind fields from the WRF forecasts, Control and QSCAT, are shown in Figure 11. Note that the maximum winds in the QSCAT experiment wind field exceed 85 kts (magenta color), similar to the H*WIND analysis, while the maximum winds in the Control experiment wind field are not as high. Finally, note that the wind fields in Figure 11 are valid at 06 UTC 13 September, 1.5 hours before the observed landfall. Note that the Control forecast has brought Ike ashore already, and Ike is still just offshore in the QSCAT experiment, in better agreement with the observed time of landfall.

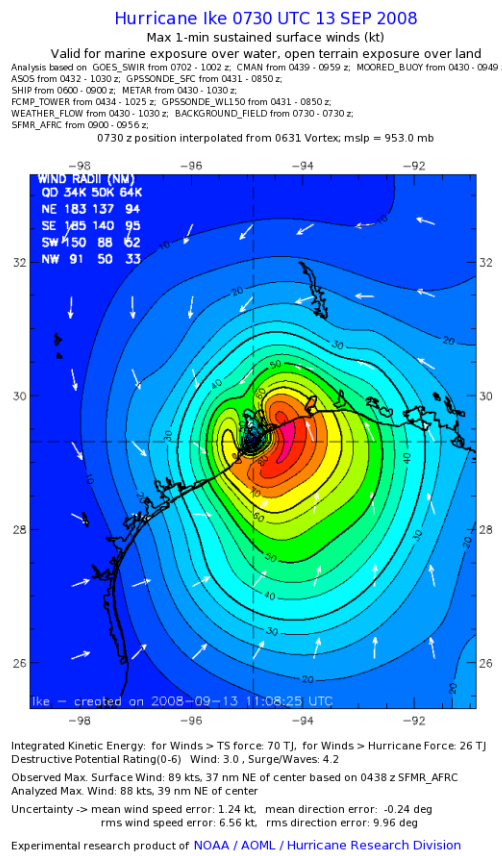

Figure 10. H*Wind analysis of Hurricane Ike at landfall. The wind speed field is colored according to wind speed, with contours every 5 knots. Bold contours are used for wind speeds of 34 kts (tropical storm), 50 kts and 64 kts (hurricane force). The vector winds are shown with white arrows.

Control

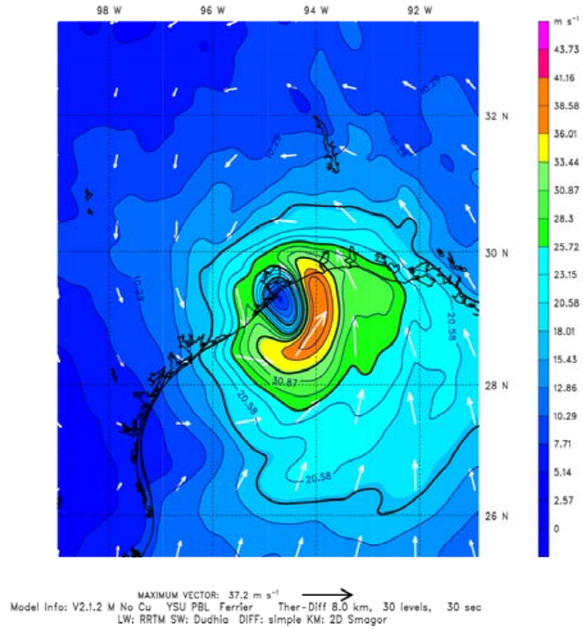

QSCAT

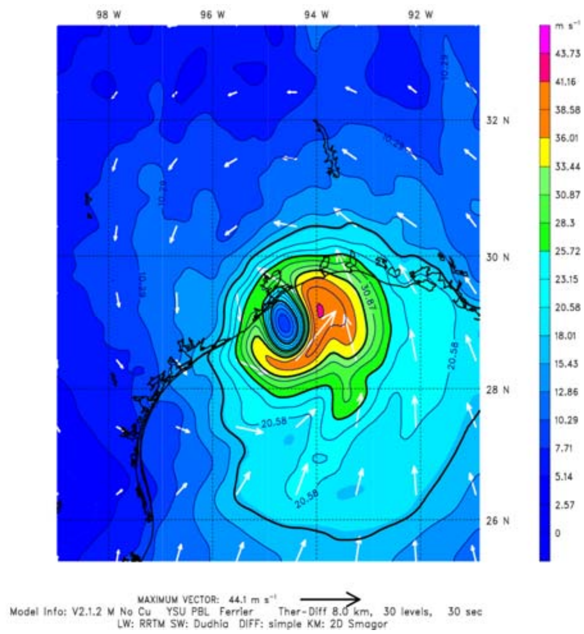

Figure 11. Surface wind field of Ike from Control (upper) and QSCAT (lower) forecasts 1.5 hours before observed landfall. Plotting convention is the same as in Fig. 10, except winds are plotted in m s^{-1}, using the same contour intervals specified in knots in the previous figure.

5. CONCLUSIONS

There is evidence from the paired global and regional data assimilation experiments presented here that

- ASCAT winds improve Hanna track forecasts in GEOS-5 and the WRF as a result of a better steering environment.
- QuikSCAT winds improve the forecast of the wind field at landfall and the timing of landfall of Hurricane Ike.
- The interaction of the GEOS-5 and WRF models suggest that scatterometer data can provide valuable information at both scales, potentially improving the forecast via two distinct mechanisms.

The scope of this study is limited to two hurricanes, and two particular data assimilation and modeling systems (GEOS-5 and WRF). Further, the positive impact of the surface winds occurred for different reasons in the two cases, so no general conclusions can be drawn at this time. However, the pairing here of a global DAS and a regional mesoscale DAS provides a realistic testbed to investigate impacts of satellite ocean surface wind data sets on hurricane forecasting. Additional experiments initiated at other times during the Hanna and Ike periods are needed to corroborate the results found thus far.

ACKNOWLGEMENTS

This work is supported by NASA Contract NNG06HX03C and contributes to NASA's Ocean Vector Winds Science Team goals. Thanks also to the staff at NASA's Center for Computational Sciences (NCCS) who supported the generation of these forecasts.

REFERENCES

Berg, R., 2009: Tropical Cyclone Report, Hurricane Ike. NHC TCR-AL092008, 55 pp.

Brown, D. J. and T. Kimberlain, 2008: Tropical Cyclone Report, Hurricane Hanna. NHC TCR-AL082008, 36 pp.

Kleist D. T., D. F. Parrish, J. C. Derber, R. Treadon, and W.-S. Wu, 2009: Introduction of the GSI into the NCEP global data assimilation system. *Wea. Forecasting*, **24,** 1691-1705.

Rienecker, M. M., M. J. Suarez, R. Todling, J. Bacmeister, L. Takacs, H.-C. Liu, W. Gu, M. Sienkiewicz, R.D. Koster, R. Gelaro, I. Stajner, and J. E. Nielsen, 2008: The GEOS-5 Data Assimilation System— Documentation of Versions 5.0.1, 5.1.0, and 5.2.0. NASA/TM–2008–104606, Vol. 27, 101 pp.

Wu, W.S., R.J. Purser, and D.F. Parrish, 2002: Three-dimensional variational analysis with spatially inhomogeneous covariances. *Mon. Wea. Rev.*, **130**, 2905–2916.